

VERIFICATION OF RAMS FORECAST SEA BREEZES AND THUNDERSTORM INITIATION OVER EAST-CENTRAL FLORIDA

Jonathan L. Case*, John Manobianco, and Allan V. Dianic
NASA Kennedy Space Center / Applied Meteorology Unit / ENSCO, Inc.

Dewey E. Harms
45th Weather Squadron, United States Air Force, Patrick AFB, FL

Paul N. Rosati
45th Space Wing, Eastern Range Safety, United States Air Force, Patrick AFB, FL

1. INTRODUCTION

This paper presents a portion of the Applied Meteorology Unit's (AMU) evaluation of the Regional Atmospheric Modeling System (RAMS) contained within the Eastern Range Dispersion Assessment System (ERDAS). ERDAS is designed to provide emergency response guidance for operations at the Cape Canaveral Air Force Station (CCAFS) and Kennedy Space Center (KSC), Florida, in the event of an accidental hazardous material release or an aborted vehicle launch. The evaluation protocol is based on the needs of 45th Space Wing/Range Safety and 45th Weather Squadron personnel, and designed to provide specific information about the capabilities, limitations, and daily operational use of RAMS in ERDAS at KSC/CCAFS.

The prognostic data from RAMS is available to ERDAS for display and input to the Hybrid Particle and Concentration Transport (HYPACT) model. The HYPACT dispersion model provides three-dimensional dispersion predictions using RAMS forecast grids. Thus, the accuracy of the HYPACT model is dependent upon the prognostic data provided by the RAMS model. This paper is organized into the following sections. Section 2 provides a brief discussion of the operational RAMS configuration in ERDAS, Section 3 describes the evaluation methodology used to verify forecast sea breezes and the daily model thunderstorm initiation, Sections 4 and 5 present the sea breeze and thunderstorm initiation verifications, respectively, and Section 6 summarizes the findings of this paper.

2. OPERATIONAL RAMS CONFIGURATION

In ERDAS, the three-dimensional, non-hydrostatic mode of RAMS is run operationally at CCAFS on four nested grids with horizontal grid spacing of 60, 15, 5, and 1.25 km, respectively (Fig. 1). The lateral boundary conditions are nudged (Davies 1983) by 12–36-h forecasts from the National Centers for Environmental Prediction 32-km Eta model that have been interpolated onto an 80-km grid. Output from the Eta model is available every six hours for boundary conditions to RAMS. Two-way interactive boundary conditions are utilized on the inner three grids. The physical parameterization schemes used in RAMS include a cloud microphysics scheme following Cotton *et al.* (1982), a modified Kuo cumulus convection scheme (Tremback 1990), the Chen and Cotton (1988) radiation scheme, a Mellor and Yamada (1982) type turbulence closure, and an 11-layer soil-

vegetation model with fixed soil moisture as the initial condition (Tremback and Kessler 1985). The modified Kuo scheme is run on grids 1–3 whereas the 1.25-km grid 4 utilizes explicit convection. The mixed-phase microphysics scheme is run on all grids.

RAMS is initialized twice-daily at 0000 and 1200 UTC using the Eta 12-h forecast grids and operationally-available observational data including the CCAFS rawinsonde, Aviation Routine Weather Reports, buoys, KSC/CCAFS wind-towers, and KSC/CCAFS 915-MHz and 50-MHz Doppler radar wind profiler data. No variational data assimilation or nudging technique is applied when incorporating observational data. Instead, RAMS is initialized from a cold start by integrating the model forward in time without using any balancing or data assimilation steps. For the initial condition, observational data are analyzed onto hybrid coordinates using the RAMS isentropic analysis package (Tremback 1990). Refer to Case *et al.* (2000) for more details on the RAMS hardware and performance characteristics.

RAMS forecast output is available once per hour for display and analysis purposes. Thus, all portions of this model verification study are limited in time to a frequency of one hour, regardless of the frequency of available observational data. This frequency of model output presents a limiting factor in the verification since warm-season weather phenomena in Florida can develop over time scales much shorter than one hour (particularly convection). Nonetheless, hourly forecast output at high spatial resolution has the potential to provide valuable guidance for short-term forecasting in east-central Florida.

3. EVALUATION METHODOLOGY

3.1 East Coast Sea Breeze Verification

The AMU conducted a subjective verification of the East Coast Sea Breeze (ECSB) within the KSC/CCAFS wind-tower network located over east-central Florida. All archived RAMS forecasts for May–August 1999 and May–September 2000 were examined. The AMU selected 12 wind towers to conduct the ECSB verification, representing three different zones in the network (the coastal barrier islands, Merritt Island, and mainland Florida, Fig. 2). In each zone, four towers were identified in a north-south orientation that contained the most data for both the 1999 and 2000 Florida warm seasons. Twelve-panel graphical plots displaying both the forecast and observed wind direction and speed were generated for all RAMS forecast cycles to verify the occurrence and timing of the ECSB at each selected tower.

*Corresponding author address: Jonathan Case, ENSCO, Inc., 1980 N. Atlantic Ave., Suite 230, Cocoa Beach, FL 32931. Email: case.jonathan@ensco.com

The AMU utilized surface observations, visible satellite imagery, and Weather Surveillance Radar, model 74C (WSR-74C) reflectivity data to identify the occurrence of the ECSB. An observed sea breeze is typically accompanied by a sharp clearing line and reflectivity fine line, which propagate westward with the sea breeze. To determine the occurrence and timing of the sea-breeze passage, the AMU examined each KSC/CCAFS wind tower for the development and maintenance of a wind-shift to an onshore component (wind direction between 335° and 155° , the approximate orientation of the Florida coastline). At wind towers 1 and 3, the wind directions representing onshore flow were expanded due to the local orientation of the coastline along the tip of the Cape (Fig. 2). Onshore flow was defined as a wind direction between 180° and 335° at tower 1 and between 200° and 335° at tower 3. As a result, both of these towers have a larger range of onshore wind directions compared to the other selected towers. Under easterly flow regimes, a sea-breeze passage was determined by an increase in the negative (easterly) u-wind at each wind tower. These same wind criteria were also applied to the ERDAS RAMS forecasts interpolated to each wind-tower location to determine the forecast ECSB passage.

The occurrence of a forecast sea breeze was verified on a per-tower basis at each selected tower. This methodology demands spatial accuracy from the model predictions and creates a large data base. However, when performing statistical comparisons of the ECSB results, the spatial correlation of errors were taken into account.

3.2 Thunderstorm Initiation Verification

A technique was developed to identify the first observed and forecast thunderstorm to the nearest hour on the RAMS innermost grid (grid 4). Grid 4 was divided into six separate zones, three coastal and three inland (Fig. 3). Forecast and observed data were examined between the hours of 1500 and 2300 UTC daily from 1 May to 30 September 2000. This time window for validation was chosen for three reasons. First, warm-season thunderstorms occur most frequently in central Florida during these hours (Reap 1994). In addition, both the 0000 and 1200 UTC RAMS forecast cycles from the same day overlap this time frame. Third, Numerical Weather Prediction (NWP) models that are cold-started without a data assimilation scheme, such as the current operational RAMS, require a “spin-up” time period (~ few hours) before the model can generate precipitation adequately (Mohanty *et al.* 1996; Takano and Segami 1993). By starting the verification window at 1500 UTC, the 1200 UTC cycle of RAMS attains a 3-h spin-up time for generating precipitation.

Archived Cloud-to-Ground Lightning Surveillance System data and visible satellite imagery were used to identify the first observed thunderstorm in each zone of RAMS grid 4 on an hourly basis. Since NWP models such as RAMS do not explicitly predict lightning and thunderstorms, an empirical technique was adopted to define a model-predicted thunderstorm. Applying results from an east-central Florida dual-Doppler observational study conducted during the Convection and Precipitation/Electrification Experiment (Yuter and Houze 1995a; Yuter and Houze 1995b), a model thunderstorm was defined by a predicted vertical velocity of 2 m s^{-1} or greater at 7-km height in conjunction with a forecast precipitation rate of at least 5 mm h^{-1} (0.2 in h^{-1}). This definition ensures that the model convection and updraft has

reached a height where mixed-phase water particles co-exist, a condition found in electrified clouds (Bringi *et al.* 1997).

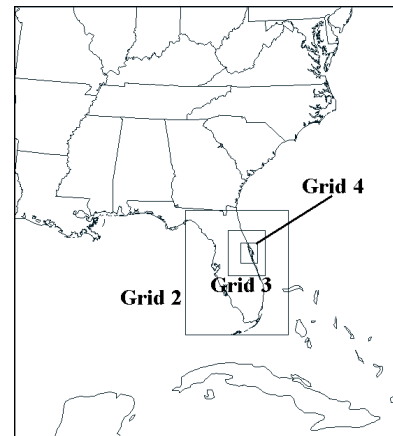


Figure 1. The real-time RAMS domains for the 60-km mesh grid (grid 1) covering the southeastern United States and adjacent coastal waters, the 15-km mesh grid (grid 2) covering the Florida peninsula and adjacent coastal waters, the 5-km mesh grid (grid 3) covering east-central Florida and adjacent coastal waters, and the 1.25-km mesh grid (grid 4) covering the area immediately surrounding KSC/CCAFS.

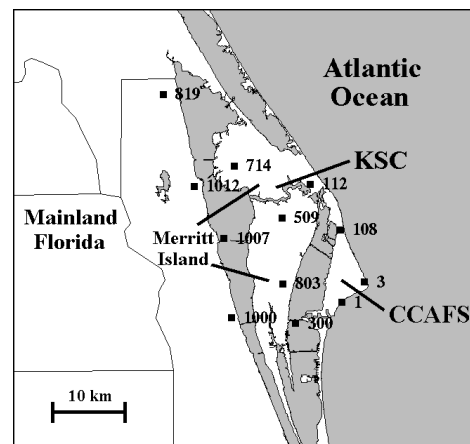


Figure 2. A map showing the locations of KSC, CCAFS, Merritt Island, and the 12 KSC/CCAFS wind towers used for the sea-breeze subjective verification. The wind towers chosen to verify the sea breeze were along the immediate Atlantic coastline, Merritt Island, and mainland Florida.

For each day that RAMS correctly predicted the occurrence of a thunderstorm within the grid-4 domain, the spatial and timing accuracy of the thunderstorm initiation were evaluated. For the spatial accuracy, the number of days were counted in which RAMS correctly predicted the location of thunderstorm initiation in one or more zones, irrespective of timing. For the timing accuracy, the number of days were counted in which RAMS correctly predicted the initiation time exactly (0-h difference between observations and forecast), within 1 h (-1 to $+1$ h error), within 2 h (-2 to $+2$ h error), and within 3 h (-3 to $+3$ h error) of the observed time, irrespective of spatial accuracy. In addition, the spatial and timing accuracy of thunderstorm initiation were examined in

combination by developing contingency tables and determining categorical and skill scores for each individual grid-4 zone based on specific timing thresholds.

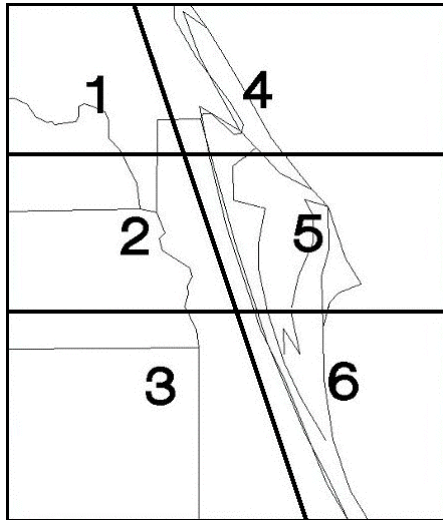


Figure 3. A plot of the 6-zone classification scheme used for the thunderstorm initiation verification during the months of May–September 2000. The division between the western (1–3) and eastern zones (4–6) is designed to parallel the Atlantic coast of central Florida.

4. SEA-BREEZE VERIFICATION

Tables 1 and 2 summarize the results of the ECSB occurrence at all 12 KSC/CCAFS wind towers in a contingency table and its associated categorical and skill scores. These tables represent nine months of data (May–August 1999 and May–September 2000) for both the 0000 and 1200 UTC RAMS forecast cycles. If no data were missing, the theoretical maximum number of elements in

Table 1 is 3312 for each forecast cycle (276 days multiplied by 12 wind towers); however, several forecasts were missing and several towers experienced various outages particularly during the 2000 warm season. In addition, when either the 0000 or 1200 UTC forecast was missing on a given day, the other forecast cycle was removed to maintain the exact same database for a statistical comparison between the two forecast cycles. As a result, about 75% (2469 elements) of the possible data are available for the evaluation.

Based on the results in Tables 1 and 2, observed sea breezes occurred at the 12 wind towers about 65% of the time (1609 out of 2469 elements), of which RAMS correctly predicted 86% of them in the 0000 UTC cycle and 98% of them in the 1200 UTC cycle, according to the Probability of Detection (POD) in Table 2. The probability of a null event (PON, not shown), the score analogous to POD for correct “no” forecasts of a sea breeze, indicates that both forecast cycles correctly predict non-sea breeze days only 66–70% of the time. The False Alarm Rate (FAR) is 16% for both the 0000 and 1200 UTC RAMS cycles. As a result of the higher POD in the 1200 UTC forecasts, this RAMS cycle has the highest Critical Success Index (CSI) and Heidke Skill Score (HSS). The HSS of 0.69 suggests that RAMS demonstrates a significant amount of utility in predicting the occurrence of the ECSB. With the exception of the FAR, each of the differences in scores between the 0000 and 1200 UTC forecasts were determined to be statistically significant, using a resampling method following Hamill (1999).

In the instances when a correct yes forecast of a sea breeze occurred, the timing errors were determined at each of the wind towers during the nine-month evaluation period. In general, the RMS error ranges from 1.5–2.1 h for each category of wind towers (not shown). The errors are smallest at the coastal towers and largest at the mainland towers, but the variation is less than 0.5 h, which is smaller than the data sampling rate of once per hour. In all instances the bias of -0.2 to -0.3 is negligible compared to the sampling rate.

TABLE 1. Contingency tables of the occurrence of the operational RAMS forecast versus observed sea breeze, verified at each of the 12 selected KSC/CCAFS towers (Fig. 2) during the 1999 and 2000 Florida warm seasons.

0000 UTC Forecast Cycle	Observed Sea Breeze	No Observed Sea Breeze
Forecast Sea Breeze	1381	261
No Forecast Sea Breeze	228	599
1200 UTC Forecast Cycle	Observed Sea Breeze	No Observed Sea Breeze
Forecast Sea Breeze	1575	293
No Forecast Sea Breeze	34	567

TABLE 2. Categorical and skill scores of RAMS forecast versus observed sea breeze during the 1999 and 2000 Florida warm seasons, associated with the contingencies in Table 1.

Parameter	0000 UTC Forecast Cycle	1200 UTC Forecast Cycle
Probability of Detection	0.86	0.98
False Alarm Rate	0.16	0.16
Bias	1.02	1.16
Critical Success Index	0.74	0.83
Heidke Skill Score	0.56	0.69

5. THUNDERSTORM INITIATION VERIFICATION

In general, both forecast cycles are comparable in terms of the spatial accuracy, whereas the 1200 UTC cycle exhibits more favorable results in the occurrence and timing of thunderstorm initiation. Table 3 summarizes the spatial and timing results of the RAMS forecast thunderstorm initiation for the 0000 and 1200 UTC cycles. Both forecast cycles correctly predicted thunderstorm initiation in one or more zones about half the time (58% in 0000 UTC cycle and 46% in 1200 UTC cycle, Table 3). The slightly poorer performance of the 1200 UTC cycle could be attributed to the larger sample size of correctly-forecast thunderstorm days (not shown). In the timing accuracy, only 8% (19%) of the correctly predicted thunderstorm days experienced an exact initiation time to the nearest hour in the 0000 UTC (1200 UTC) cycle. Meanwhile, RAMS correctly predicted the hourly thunderstorm initiation time to within 3 hours of the observed time about 75% of all days for both forecast cycles (slightly higher in the 1200 UTC forecasts). The timing RMS errors of thunderstorm initiation anywhere on RAMS grid 4 were generally between 2–3 h for both forecast cycles whereas the bias was about 1 h in the 0000 UTC cycle and 0 h in the 1200 UTC cycle (not shown). The timing error statistics for thunderstorm initiation in each individual grid-4 zone did not exhibit any trends or organized patterns that favored specific zones. Note that these timing errors in RAMS do not reflect off-hour predictions because forecast output was available only at the top of each hour.

Figure 4 shows the POD and FAR scores of the thunderstorm occurrence for both RAMS cycles as a function of grid-4 zone and timing thresholds. In all six zones, the 0000 UTC POD is less than 0.40 under all timing thresholds whereas the FAR is typically larger than the POD (Figs. 4a and b). These results suggest that the 0000 UTC forecast cycle has limited value in predicting the occurrence of thunderstorms anywhere on grid 4. The 1200 UTC forecast cycle shows marked improvement over the 0000 UTC cycle, since the POD scores are typically higher by a factor of two or more (Figs. 4a and c). However, the FAR scores are still quite high, especially when verifying RAMS predicted thunderstorm initiation to the nearest hour ($FAR > 0.4$ in Fig. 4d). Considering the cold-start initialization, these results indicate that a more recent initialization of RAMS is important in improving the model's ability to predict thunderstorm initiation.

These results suggest that the more recent initialization of RAMS (1200 UTC) to the time of convection initiation improves the predictions of the occurrence of thunderstorms, but does not considerably improve the accuracy of the

predicted location and timing of thunderstorm initiation. This somewhat limited skill in the predicted location and timing of thunderstorm initiation could be related to four characteristics of the current RAMS configuration.

- The lateral boundaries of grid 4, particular the eastern boundary, are not sufficiently displaced from the area of interest (e.g. the Florida east coast). Expansion of grid 4 could alleviate the negative impacts and errors that can be caused by lateral boundary interactions with the coarser grid, especially in zone 6 (Warner *et al.* 1997).
- Errors in precipitation and the vertical distribution of latent heating, associated with the parameterized treatment of convection on the outer grids, greatly impact the explicit convective forecasts on the inner grid (Warner and Hsu 2000). In fact, Warner and Hsu (2000) found that different precipitation parameterizations on the outer grids produced up to a factor of 3 difference in their 24-h precipitation forecasts.
- Soil moisture data are not ingested into RAMS nor initialized based on previous rainfall. Horizontal variations in soil moisture resulting from past rainfall events can play an important role in determining the favored locations of convective initiation. The combination of ingesting soil moisture observations and running an antecedent precipitation index algorithm using previous rainfall data can result in a more accurate soil moisture initial condition for RAMS.
- A more sophisticated mesoscale initialization and data assimilation scheme than the current cold-start initialization is needed for RAMS, where high-resolution, continuous observational data such as Doppler radar and satellite data are assimilated and brought into balance with the model equations.

6. SUMMARY

This paper presented subjective model verification results of RAMS as run operationally within ERDAS. The ECSB verification was performed for the 1999 and 2000 Florida warm seasons, and the daily thunderstorm initiation was conducted during the 2000 warm season.

The ECSB occurrence and timing was verified at 12 selected KSC/CCAFS wind towers in east-central Florida to represent the sea-breeze passage at coastal locations, Merritt Island, and mainland Florida. Thunderstorm initiation was verified by using observed cloud-to-ground lightning data and defining a model-predicted thunderstorm based on sufficient upward vertical velocity in the mixed-phase portion of a cloud in combination with model-generated precipitation.

TABLE 3. A list of the number and percent of days that RAMS correctly identified one or more of the grid-4 zones for thunderstorm initiation, the number and percent of days that RAMS correctly predicted thunderstorm initiation to the nearest hour, within 1 hour (± 1 hour), within 2 hours (± 2 hours), and within 3 hours (± 3 hours). The total is based on the number of correctly-predicted thunderstorm days.

Parameter	0000 UTC Cycle			1200 UTC Cycle		
	Number	Total	% Correct	Number	Total	% Correct
≥ 1 zone correct	21	36	58	29	63	46
Correct timing	3	36	8	12	63	19
Timing within 1 h	13	36	36	26	63	42
Timing within 2 h	19	36	53	38	63	61
Timing within 3 h	26	36	72	48	63	77

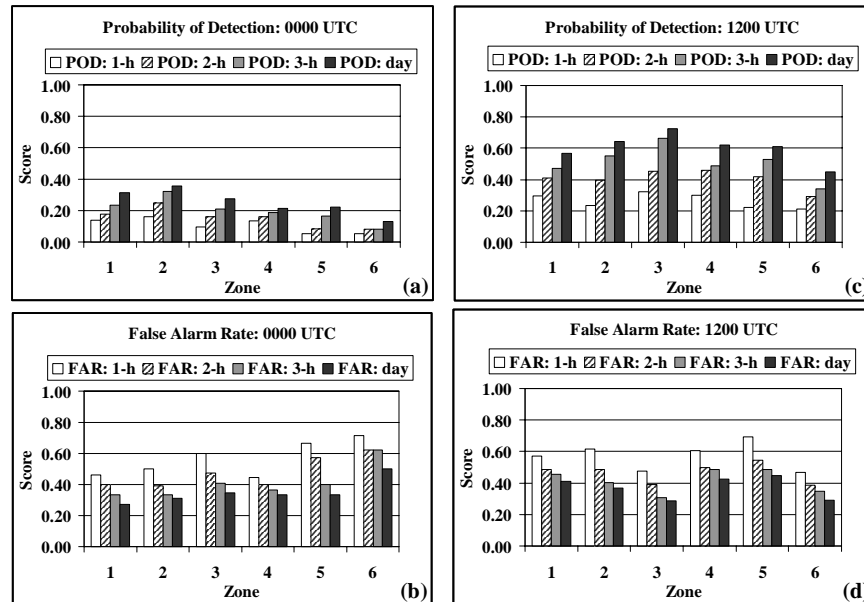


Figure 4. The Probability of Detection (POD) and False Alarm Rate (FAR) for the RAMS 0000 and 1200 UTC forecasts of the first daily thunderstorm occurrence in each zone of grid 4 during the hours of 1500–2300 UTC. The 0000 UTC POD and FAR are shown in a) and b) respectively, and the 1200 UTC POD and FAR are shown in c) and d) respectively. The scores were determined by verifying hourly RAMS thunderstorm occurrences to the nearest 1 h, 2 h, 3 h, and for the entire daily verification period according to the scale provided.

The results in this paper suggest that the operational RAMS at CCAFS is an excellent predictor of the ECSB in central Florida. However, RAMS demonstrated somewhat limited skill in predicting the timing and location of thunderstorm initiation across the innermost RAMS forecast grid. The limited skill in thunderstorm forecasts could be amended by modifying the current configuration and cycling strategy of RAMS in ERDAS. For a copy of the final report on the RAMS evaluation, please contact the corresponding author listed in this paper.

7. REFERENCES

- Brangi, V. N., K. Knupp, A. Detwiler, L. Liu, I. J. Caylor, and R. A. Black, 1997: Evolution of a Florida thunderstorm during the Convection and Precipitation/Electrification Experiment: The case of 9 August 1991. *Mon. Wea. Rev.*, **125**, 2131-2160.
- Case, J. L., J. Manobianco, A. V. Dianic, D. E. Harms, and P. N. Rosati, 2000: A sensitivity and benchmark study of RAMS in the Eastern Range Dispersion Assessment System. Preprints, *9th Conf. on Aviation, Range, and Aerospace Meteorology*, 11-15 September 2000, Orlando, FL, Amer. Meteor. Soc., 426-431.
- Chen, S., and W. R. Cotton, 1988: The sensitivity of a simulated extratropical mesoscale convective system to longwave radiation and ice-phase microphysics. *J. Atmos. Sci.*, **45**, 3897-3910.
- Cotton, W. R., M. A. Stephens, T. Nehrkorn, and G. J. Tripoli, 1982: The Colorado State University three-dimensional cloud/mesoscale model — 1982. Part II: An ice phase parameterization. *J. de Rech. Atmos.*, **16**, 295-320.
- Davies, H. C., 1983: Limitations of some common lateral boundary schemes used in regional NWP models. *Mon. Wea. Rev.*, **111**, 1002-1012.
- Hamill, T. M., 1999: Hypothesis tests for evaluating numerical precipitation forecasts. *Wea. Forecasting*, **14**, 155-167.
- Mellor, G. L., and T. Yamada, 1982: Development of a turbulence closure model for geophysical fluid problems. *Rev. Geophys. Space Phys.*, **20**, 851-875.
- Mohanty, U. C., A. Kasahara, and R. Errico, 1986: The impact of diabatic heating on the initialization of a global forecast model. *J. Meteor. Soc. Japan*, **64**, 805-817.
- Reap, R. M., 1994: Analysis and prediction of lightning strike distributions associated with synoptic map types over Florida. *Mon. Wea. Rev.*, **122**, 1698-1715.
- Takano, I. and A. Segami, 1993: Assimilation and initialization of a mesoscale model for improved spin-up of precipitation. *J. Meteor. Soc. Japan*, **71**, 377-391.
- Tremback, C. J., 1990: Numerical simulation of a mesoscale convective complex: model development and numerical results. Ph.D. Dissertation, Atmos. Sci. Paper No. 465, Department of Atmospheric Science, Colorado State University, Fort Collins, CO 80523, 247 pp.
- Tremback, C. J., and R. Kessler, 1985: A surface temperature and moisture parameterization for use in mesoscale numerical models. Preprints, *7th AMS Conf. on Numerical Weather Prediction*, June 17-20, Montreal, Quebec, Amer. Meteor. Soc., Boston, MA, 355-358.
- Warner, T. T., R. A. Peterson, and R. E. Treadon, 1997: A tutorial on lateral boundary conditions as a basic and potentially serious limitation to regional numerical weather prediction. *Bull. Amer. Meteor. Soc.*, **78**, 2599-2617.
- _____, and H-M. Hsu, 2000: Nested-model simulation of moist convection: The impact of coarse-grid parameterized convection on fine-grid resolved convection. *Mon. Wea. Rev.*, **128**, 2211-2231.
- Yuter, S. E., and R. A. Houze Jr., 1995a: Three-dimensional kinematic and microphysical evolution of Florida cumulonimbus. Part I: Spatial distribution of updrafts, downdrafts, and precipitation. *Mon. Wea. Rev.*, **123**, 1921-1940.
- _____, and _____, 1995b: Three-dimensional kinematic and microphysical evolution of Florida cumulonimbus. Part II: Frequency distributions of vertical velocity, reflectivity, and differential reflectivity. *Mon. Wea. Rev.*, **123**, 1941-1963.